Executive Summary Report
for ESA cont. 4000117911/16/NL/FE
“Process Development for Ultra-Thin Solar Cells”

AZUR SPACE Solar Power GmbH

D-74072 Heilbronn
Germany

Datensicherheit / *Privacy*	Schutzvermerk gemäß DIN ISO 16016 beachten / *All rights reserved /copy rights per DIN ISO 16016*

		Name	Date	Signature	
Prepared	TC	C. Noumissing Sao	2019-09-02		
	TC	Wolfgang Köstler	2019-09-10		**TP 0006078-01**
Approved	T	Dr. Gerhard F.X. Strobl	2019-09-10		
Released	B	Dr. Wolfgang Guter	2019-09-10		
Dateiname / File					

© AZUR SPACE Solar Power GmbH

1 Introduction

The main purpose of this contract was to manufacture and test ultrathin lightweight space solar cells which are based on the epitaxial growth of III-V semiconductors on Ge and GaAs substrates, respectively. One incentive was the development of ultrathin, lightweight cells. Another incentive was the potential reuse of the growth substrates for cost reduction. Ultrathin solar cell layers were lifted from the substrates, based on using two different lift-off techniques: Epitaxial lift-off (ELO) and spalling. In the spalling process, stressor layers are used for lifting upright structures together with a germanium bottom cell. This part was covered by AZUR SPACE. Fraunhofer ISE has developed and manufactured the epitaxial structures for the ELO process. For the ELO process, which was covered by tf2 devices B.V., a sacrificial layer (AlAs) is used between substrate and epitaxial layers (inversely grown epitaxial structures) which is laterally etched away, enabling the separation of the two.

2 Results

For the layer release by spalling, we have used the application of metal layers by sputtering and electroplating, respectively. We have investigated two release concepts, spalling and exfoliation, which differ in the methods for crack initiation and crack propagation through the substrate. We have applied the release concepts to lattice-matched 3G30 and UMM 4G32 wafers. Spalling in combination with 3G30 produced the best results, so we have selected this route for the manufacturing of samples. After the layer release, the ultrathin layers were temporarily bonded to handling substrates. The solar cell processing included the formation of front and rear contacts, antireflective coating and cell separation. Image 1 shows an ultrathin solar cell wafer after processing, separated on wafer level into different cell sizes between 1 cm² and 30.18 cm². The thickness of the cells is about 30 µm.

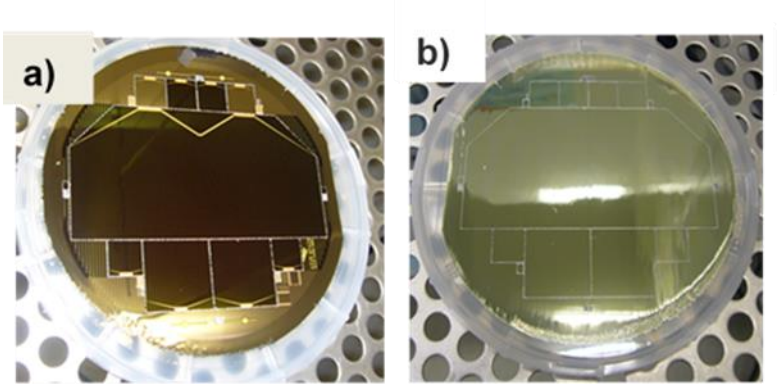

Img. 1: 3G30 solar cell wafer after processing. a) Front side. b) Rear side

© AZUR SPACE Solar Power GmbH

We have also produced solar cell assemblies (SCAs) from the ultrathin cells. We have developed a welding procedure which provides good adhesion and does not damage the ultrathin cell and have also adapted the application of cover glasses. AZUR has also developed welding and cover glassing for ELO cells as described below. Image 2 shows a tray with eight ultrathin 3G30 SCAs.

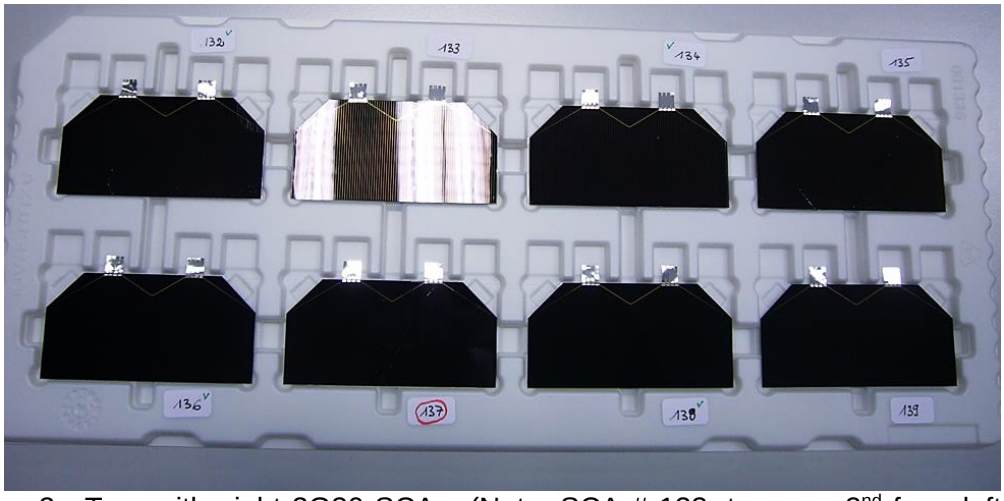

Img. 2: Tray with eight 3G30 SCAs. (Note: SCA # 133, top row, 2nd from left, shows a reflection of the fluorescent lamp room lighting.)

We found that the efficiency of the ultrathin SCAs was lower compared to reference cells from AZUR's production line. One reason for this is that the germanium substrate, which also forms the bottom cell of the triple junction solar cell, is only 20 to 25 µm thick. Electrical characterization results are presented in table 2 in combination with thermal cycling.

Fraunhofer ISE has investigated the epitaxy process stability and manufacturability of inverted triple junction solar cells by supplying epitaxial inverted metamoprhic triple junction wafers for ELO.

tf2 has developed ELO for inverted metamorphic triple junction (IMM3J) layer structures. This resulted in a trend of increasing ELO yield, with 80% yield being approached, as illustrated in Image 3 (left). An example of a damage-free IMM3J ELO film is depicted in Image 3 (right).

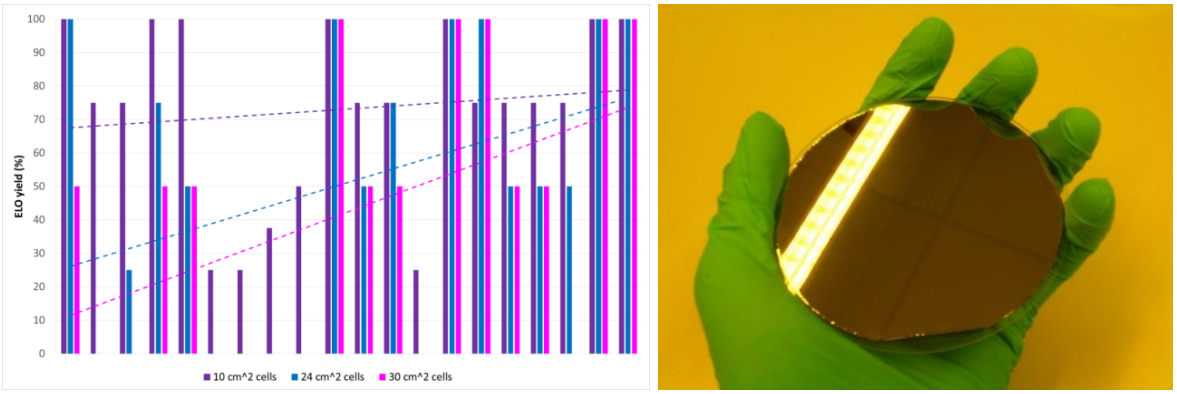

Img. 3 Left: ELO yield for a series of consecutive runs. The dotted lines are linear fits to the data. Right: Damage-free ultra-thin 4" IMM3J ELO film mounted on a rigid carrier.

The ultra-thin cell processing of the IMM3J ELO structures was also developed. Cell processing yield for large area solar cells was increased significantly. In collaboration with ISE, the AM0 EOL

© AZUR SPACE Solar Power GmbH

current matching was improved as well. A schematic presentation of the resulting manufacturing process is provided in Image 4 (left).

The following functioning free-standing IMM3J ELO solar cell sizes were manufactured: 10 cm^2 24 cm^2 and 30 cm^2. Note that the 24 and 30 cm^2 cells are significantly larger than the largest IMM3J ELO cells (20.6 cm^2) reported in the literature. 30 cm^2 IMM3J ELO cells are presented in Image 4 (right). Notice that the (flexible) free-standing IMM3J cells are warped.

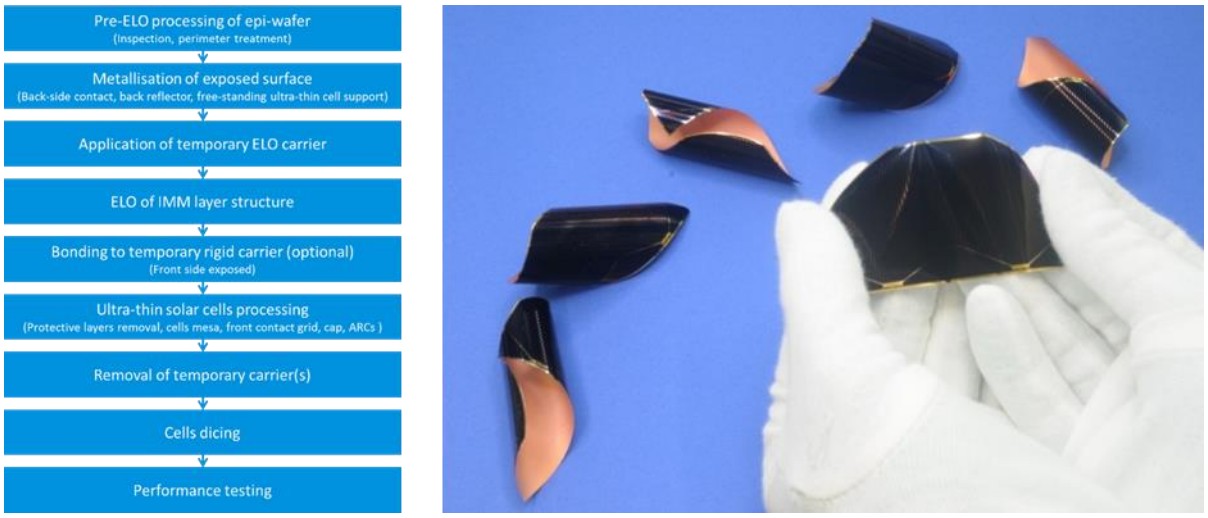

Image 4: Left: Process flow for free-standing ultra-thin IMM3J ELO solar cells. Right: Free-standing 30 cm^2 IMM3J ELO solar cells.

IV- and QE-curves of the manufactured 30 cm^2 IMM3J ELO cells are presented in Image 5. The Jsc_AM0 values are determined from the EQE curves. The Voc values of all the IMM3J ELO cells are close to that of the non-ELO reference and to values of similar IMM3J cells presented in the literature. Together with the fact that the curves generally demonstrate a high shunt resistance this indicates that the ultra-thin ELO films are of a high quality. The FF is lower than typical literature values (85-87.5%) for similar IMM3J cells. It can be improved with a more optimised front contact grid design and thickness, and improvements in the cell mesa etch. The Jsc is also below or at the bottom end of typical literature values (16-17.4 mA/cm^2) for similar IMM3J cells. Further improvements in subcell current matching and ARCs can increase the Jsc. Note, however, that the layer structure was always optimised for optimum efficiency (i.e. current matching) at EOL, not BOL. The maximum efficiency obtained was 28.0% for a 24 cm^2 cell. Although there is room for improvement, the obtained efficiencies in combination with the cell masses result in impressive numbers for areal mass density and specific power, as presented in table 1.

Table1: Additional IMM3J ELO solar cell parameters for cells with a standard support

Cell area (cm^2)	10.00	24.37	30.00
Metal support area (cm^2)	11.4	26.3	31.4
Mass (mg)	199 ± 5	451 ± 9	537 ± 17
Efficiency (%)	23.6 ± 1.1	27.1 ± 0.7	26.4 ± 1.6
Areal mass density (mg/cm^2)	19.9 ± 0.5	18.5 ± 0.4	17.9 ± 0.6
Specific power (mW/g)	1623 ± 80	2001 ± 60	2029 ± 150

© AZUR SPACE Solar Power GmbH

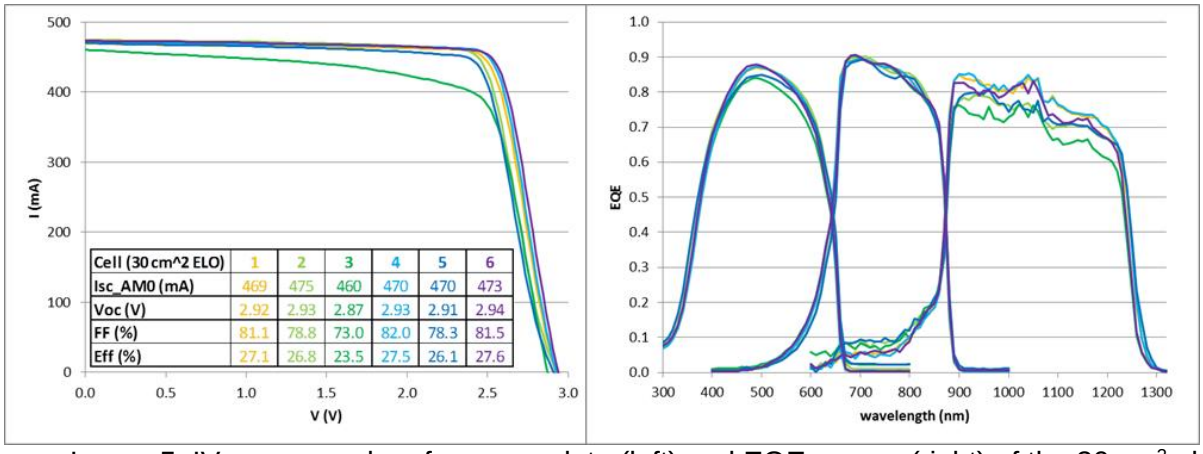

Image 5: IV-curves and performance data (left) and EQE-curves (right) of the 30 cm² ultra-thin IMM3J ELO cells. The IV-curves are scaled to match the AM0 Isc values determined from the corresponding EQE measurements, while keeping Voc constant.

Despite the curvature of the ELO cells, AZUR demonstrated the welding and cover glassing of 10 cm² ELO cells. Image 6 shows such an SCA.

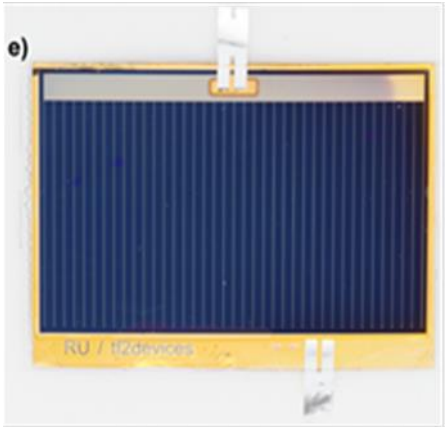

Image 6: 10 cm² SCA from ELO

Ultrathin 30.18 cm² 3G30 SCAs and 10 cm² ELO SCAs were subjected to a test program which included thermal cycling with 3 x 150 cycles from -80°C to 150°C, followed by 1000 cycles from -170°C to 100°C.

Electroluminescence imaging after thermal cycling confirmed the mechanical integrity of all SCAs, which means that the cycles did not cause any delamination, disintegration or cracking of the layers.

The results of the electrical characterization after thermal cycling are presented in table 2 and table 3 and show that the Isc of 4x8 cm² AZUR SCAs after 1000 cycles are slightly lower than the values without thermal cycling and higher than the values after 450 cycles. However, the fill factor increases slightly compared to the measurement before cycling, which also results in an improved efficiency. We assume that the explanation of the increase is a mitigation of micro-shunts which were present in the samples before thermal cycling. tf2 ELO SCAs exhibit a slight increase in Isc and efficiency after the first 450 cycles, but also a certain degradation during the following 1000 cycles.

© AZUR SPACE Solar Power GmbH

Table 2: Electrical characterization of 30.18 cm² AZUR 3G30 SCAs after thermal cycling.

SCA No.	Isc	Voc	Imp	Vmp	Pmp	FF	eta	Cycle Nr.
4x8cm²	mA	V	mA	V	mW		%	
124	514.8	2.445	484.0	2.145	1038.2	0.82	25.17	0 cycle
	506.7	2.462	484.6	2.157	1045.4	0.84	25.34	450 cycles (III)
	-1.6	0.7	0.1	0.6	0.7	1.6	0.7	Δ(III-0) [%] *
	513	2.463	496.4	2.136	1060.4	0.84	25.71	1000 cycles (IV)
	1.3	*0.0*	*2.4*	*-1.0*	*1.4*	*0.2*	*1.4*	*Δ(IV-III) [%] **
125	513.6	2.412	482.9	1.986	959.0	0.77	23.25	0 cycle
	502.2	2.475	476.6	2.202	1049.3	0.84	25.44	450 cycles (III)
	-2.2	*2.6*	*-1.3*	*10.9*	*9.4*	*9.0*	*9.4*	*Δ(III-0) [%]*
	512.8	2.471	485.9	2.183	1060.9	0.84	25.72	1000 cycles (IV)
	2.1	*-0.2*	*2.0*	*-0.9*	*1.1*	*0.0*	*1.1*	*Δ(IV-III) [%]*
126	508.3	2.464	488.8	2.088	1020.7	0.82	24.74	0 cycle
	513.3	2.506	489.3	2.200	1076.6	0.84	26.10	450 cycles (III)
	1.0	*1.7*	*0.1*	*5.4*	*5.5*	*2.7*	*5.5*	*Δ(III-0) [%]*
	510.9	2.471	478	2.164	1034.3	0.82	25.07	1000 cycles (IV)
	-0.5	-1.4	-2.3	-1.6	-3.9	-2.0	-3.9	*Δ(IV-III) [%]*
128	512.9	2.462	493.9	2.058	1016.5	0.80	24.64	0 cycle
	510.8	2.493	495.5	2.184	1082.2	0.85	26.24	450 cycles (III)
	-0.4	*1.3*	*0.3*	*6.1*	*6.5*	*5.6*	*6.5*	*Δ(III-0) [%]*
	510.4	2.477	494.8	2.202	1088.1	0.86	26.38	1000 cycles (IV)
	-0.1	*-0.6*	*-0.1*	*0.8*	*0.5*	*1.2*	*0.6*	*Δ(IV-III) [%]*
129	512.7	2.452	485.2	2.036	987.9	0.79	23.95	0 cycle
	511.6	2.487	474.8	2.197	1043.2	0.82	25.29	450 cycles (III)
	-0.2	*1.4*	*-2.1*	*7.9*	*5.6*	*4.4*	*5.6*	Δ(III-0) [%]
	509.7	2.471	480.7	2.168	1042.4	0.83	25.27	1000 cycles (IV)
	-0.4	*-0.6*	*1.2*	*-1.3*	*-0.1*	*1.2*	*-0.1*	*Δ(IV-III) [%]*

*) Δ(III-0) is the relative variation between cycle IV and cycle 0
**) Δ(IV-III) is the relative variation between cycle IV and cycle III

Table 3: Electrical characterization of tf2 SCAs 2.5x4 cm² after thermal cycling

SCA No.	Isc	Voc	Imp	Vmp	Pmp	FF	eta	Cycle Nr.
2.5x4cm²	mA	V	mA	V	mW		%	
5	134.6	2.851	127.1	2.494	317.1	0.83	23.19	0 cycle
	140.6	2.818	132.7	2.449	325.1	0.82	23.78	450 cycles (III)
	4.4	*-1.1*	*4.4*	*-1.8*	*2.5*	*-0.7*	*2.5*	Δ(III-0) [%] *
	132.3	2.820	124.0	2.446	303.4	0.81	22.20	1000 cycles (IV)
	-5.9	*0.1*	*-6.6*	*-0.1*	*-6.7*	*-0.9*	*-6.7*	*Δ(IV-III) [%] **
7	138.3	2.869	132.1	2.570	339.4	0.86	24.83	0 cycle
	145.2	2.850	140.2	2.529	354.6	0.86	25.94	450 cycles (III)
	5.0	*-0.7*	*6.2*	*-1.6*	*4.5*	*0.2*	*4.5*	Δ(III-0) [%]
	141.5	2.855	135.4	2.534	343.1	0.85	25.10	1000 cycles (IV)
	-2.5	*0.2*	*-3.4*	*0.2*	*-3.3*	*-1.0*	*-3.3*	*Δ(IV-III) [%]*
11	136.5	2.866	128.6	2.554	328.5	0.84	24.03	0 cycle
	145.7	2.836	137.8	2.499	344.4	0.83	25.19	450 cycles (III)
	6.7	*-1.1*	*7.1*	*-2.1*	*4.8*	*-0.8*	*4.8*	Δ(III-0) [%]
	140.3	2.845	132.4	2.518	333.3	0.83	24.38	1000 cycles (IV)
	-3.7	*0.3*	*-3.9*	*0.7*	*-3.2*	*0.1*	*-3.2*	*Δ(IV-III) [%]*
12	133.5	2.883	128.5	2.591	332.8	0.87	24.35	0 cycle
	142.0	2.861	136.0	2.552	347.1	0.85	25.39	450 cycles (III)
	6.4	*-0.7*	*5.9*	*-1.5*	*4.3*	*-1.3*	*4.3*	Δ(III-0) [%]
	135.7	2.870	130.2	2.574	335.0	0.86	24.51	1000 cycles (IV)
	-4.5	*0.3*	*-4.3*	*0.8*	*-3.5*	*0.7*	*-3.5*	*Δ(IV-III) [%]*
14	140.2	2.874	133.5	2.545	339.9	0.84	24.86	0 cycle
	145.8	2.863	139.4	2.520	351.3	0.84	25.70	450 cycles (III)
	4.1	*-0.4*	*4.4*	*-1.0*	*3.4*	*-0.3*	*3.4*	Δ(III-0) [%]
	141.4	2.872	134.2	2.537	340.4	0.84	24.90	1000 cycles (IV)
	-3.0	*0.3*	*-3.7*	*0.7*	*-3.1*	*-0.4*	*-3.1*	*Δ(IV-III) [%]*
20	136.6	2.865	123.6	2.567	317.3	0.81	23.21	0 cycle
	141.9	2.856	129.9	2.545	330.6	0.82	24.18	450 cycles (III)
	3.8	*-0.3*	*5.1*	*-0.9*	*4.2*	*0.7*	*4.2*	Δ(III-0) [%]
	138.2	2.854	123.6	2.547	314.7	0.80	23.02	1000 cycles (IV)
	-2.5	*-0.1*	*-4.9*	*0.1*	*-4.8*	*-2.2*	*-4.8*	*Δ(IV-III) [%]*
SCA-D10	141.2	1.598	133.3	1.293	172.3	0.76	12.61	0 cycle
	145.2	1.619	136.9	1.279	175.2	0.74	12.81	450 cycles (III)
	2.9	*1.3*	*2.7*	*-1.0*	*1.6*	*-2.5*	*1.6*	Δ(III-0) [%]
	141.5	1.602	130.5	1.274	166.3	0.73	12.17	1000 cycles (IV)
	-2.6	*-1.1*	*-4.7*	*-0.4*	*-5.1*	*-1.5*	*-5.1*	*Δ(IV-III) [%]*
SCA-D14	141.4	2.845	114.9	2.514	288.9	0.72	21.13	0 cycle
	146.2	2.838	123.2	2.489	306.6	0.74	22.43	450 cycles (III)
	3.4	*-0.3*	*7.2*	*-1.0*	*6.1*	*2.9*	*6.1*	Δ(III-0) [%]
	138.7	2.833	121.6	2.498	303.8	0.77	22.22	1000 cycles (IV)
	-5.1	*-0.2*	*-1.3*	*0.4*	*-0.9*	*4.6*	*-0.9*	*Δ(IV-III) [%]*

*) Δ(III-0) is the relative variation between cycle IV and cycle 0
**) Δ(IV-III) is the relative variation between cycle IV and cycle III

© AZUR SPACE Solar Power GmbH

Conclusion:

AZUR, Fraunhofer ISE and tf2 demonstrated the release of ultrathin solar cell layers by different approaches. For both technologies, ELO and mechanical splitting, we have achieved a considerable progress over the duration of the program, with regard to reproducibility, processing time and yield. Fraunhofer ISE achived high epitaxial layer quality and homogeneity for ELO, which is confirmed by the resulting cell performance.

AZUR and tf2 were also able to demonstrate the manufacturing of large area cells and SCAs after the ultrathin layer release. Notably, AZUR succeeded in manufacturing SCAs from ultrathin, delicate, heavily curved bare cells provided by tf2. The activity included a test program with thermal cycles in order to assess the stability of the cells. Although the low number of samples and their specific properties limit the interpretation of the results, we can conclude that the cells are relatively stable in general.

The biggest achievement of the activity is that we have gained an enormous know-how on the handling and processing of ultrathin layers. We have developed new methods and implemented special processes and materials. We have adapted existing equipment and designed and build entirely new tooling. This know-how concerns virtually every processing step from the wafer to the SCA. We also learned what is important for ultrathin cell characterization and testing. What we learned is not limited to the layer release techniques explored for this contract, but is universally applicable to ultrathin cell manufacturing. This is of enormous value for future thin cell development.

© AZUR SPACE Solar Power GmbH